Indian J Med Res 142, December 2015, pp 747-758
DOI:10.4103/0971-5916.174568

Culture & differentiation of mesenchymal stem cell into osteoblast on degradable biomedical composite scaffold: *In vitro* study

Krishan G. Jain[1], Sujata Mohanty[1], Alok R. Ray[2], Rajesh Malhotra[3] & Balram Airan[4]

[1]Stem Cell Facility, [3]Department of Orthopedics and [4]Department of CTVS, All India Institute of Medical Sciences & [2]Centre for Biomedical Engineering, IIT-Delhi, New Delhi, India

Received September 21, 2013

***Background & objectives*: There is a significant bone tissue loss in patients from diseases and traumatic injury. The current autograft transplantation gold standard treatment has drawbacks, namely donor site morbidity and limited supply. The field of tissue engineering has emerged with a goal to provide alternative sources for transplantations to bridge this gap between the need and lack of bone graft. The aim of this study was to prepare biocomposite scaffolds based on chitosan (CHT), polycaprolactone (PCL) and hydroxyapatite (HAP) by freeze drying method and to assess the role of scaffolds in spatial organization, proliferation, and osteogenic differentiation of human mesenchymal stem cells (hMSCs) *in vitro*, in order to achieve bone graft substitutes with improved physical-chemical and biological properties.**

***Methods*: Pure chitosan (100CHT) and composites (40CHT/HAP, 30CHT/HAP/PCL and 25CHT/HAP/PCL scaffolds containing 40, 30, 25 parts per hundred resin (phr) filler, respectively) in acetic acid were freeze dried and the porous foams were studied for physicochemical and *in vitro* biological properties.**

***Results*: Scanning electron microscope (SEM) images of the scaffolds showed porous microstructure (20-300 µm) with uniform pore distribution in all compositions. Materials were tested under compressive load in wet condition (using phosphate buffered saline at *p*H 7.4). The *in vitro* studies showed that all the scaffold compositions supported mesenchymal stem cell attachment, proliferation and differentiation as visible from SEM images, [3-(4,5-dimethylthiazole-2-yl)-2,5-diphenyltetrazolium bromide] (MTT) assay, alkaline phosphatase (ALP) assay and quantitative reverse transcription (qRT)-PCR.**

***Interpretation & conclusions*: Scaffold composition 25CHT/HAP/PCL showed better biomechanical and osteoinductive properties as evident by mechanical test and alkaline phosphatase activity and osteoblast specific gene expression studies. This study suggests that this novel degradable 3D composite may have great potential to be used as scaffold in bone tissue engineering.**

Key words Chitosan - hydroxyapatite - polycaprolactone - scaffold - stem cell - tissue engineering

Critical size bone defects (CSD) resulting from infections, tumours, trauma, biochemical disorders and abnormal skeletal development pose significant health problems[1]. The current, gold standard therapy relies on the transplantation of autograft or allograft into the CSD[2]. The use of autograft can result in additional surgery, pain and cost to the patient. On the other hand allografts can result in disease transmission and potential immune rejection[3,4]. The use of engineered tissues can avoid some of these issues, such as the need for donor tissue, immune rejection and additional surgery by transplanting degradable biomaterial scaffolds seeded with stem cells into the injury site[1]. A tissue engineered scaffold is highly promising graft material for management of critical size bone defects resulting from infections, tumours or trauma. An ideal scaffold provides optimum micro-environment for cell and tissue in-growth and healing, supports surrounding tissue until a mature tissue is formed and replaces it[5,6]. Composites of biodegradable polymers using chitosan (CHT), poly-e-caprolactone (PCL) and hydroxyapatite (HAP) have been examined as scaffolds for their applications in bone tissue engineering[7]. CHT, a derivative of chitin is considered appropriate material for bone tissue engineering applications because of its structural similarity with glycosaminoglycan, high biocompatibility, biodegradability and osteoinductive properties[8]. The amino groups and hydroxyl groups in its backbone not only render chitosan hydrophilic feature but also make chitosan weakly basic[9]. In solution form, the amine group protonates and provides a net positive charge on chitosan. The cationic nature of this polyelectrolyte is critical to its coagulating nature and interaction with negatively charged serum proteins, collagen and glycosaminoglycan present in the extracellular matrix of cells[10]. In spite of its general acceptance as a tissue biocompatible material, chitosan is mechanically weak and degradable, and unable to maintain its shape for transplantation as a result of swelling[11]. Poly(e-caprolactone) (PCL) is a synthetic biodegradable aliphatic polyester for hard tissue regeneration due to its physical, chemical and mechanical characteristics, easy processability, tissue compatibility and low cost. It is a low modulus thermoplastic elastomer with higher toughness at room temperature [glass transition temperature, *T*g: (–)60°C][12]. Although PCL is not osteoconductive, its composite scaffold with CHT and HAP can have osteoconductive and osteoinductive potential. HAP [Ca_{10} $(PO4)_6$ $(OH)_2$] is a major mineral component of bone that makes it an attractive material in both orthopaedic and dental fields[13,14]. It is an osteoconductive material and has been used as a filler to reinforce the mechanical properties of the scaffolds[15]. It is a bioactive material which induces cell attachment, proliferation and differentiation by increasing surface roughness and thereby absorption of the proteins from surrounding environment[16].

In view of their mutual complementary properties, we combined CHT, HAP and PCL to prepare 3D biomedical composite scaffolds with desired properties. Further, stem cells or osteoblasts may be attached to the scaffold surface, or may be seeded into the scaffold before implantation[17,18]. Mesenchymal stem cells (MSCs) have been isolated from different tissues of the body[19] and can be easily harvested from bone marrow (BM) by a minor invasive clinical procedure. MSCs have the capacity of proliferation and differentiation into osteoblasts, chondrocytes, adipocytes and other tissues of mesodermal origin[20]. The focus of this study was to prepare and characterize the physical and mechanical properties of the scaffolds and to analyse their bio-suitability by seeding MSCs onto them in an *in vitro* study. In this study, micro porous 3D organic-inorganic composite scaffolds with four different compositions were prepared by freeze drying method. The pore size and porosity of scaffolds were assessed by scanning electron microscopy (SEM) and liquid displacement method. Mechanical strength and *in vitro* enzymatic degradation of these scaffolds were also investigated. MSCs were used as cell model to study the attachment, toxicity, proliferation and differentiation on scaffolds.

Material & Methods

The study was conducted in the Stem Cell Facility, All India Institute of Medical Sciences (AIIMS), New Delhi, India, after obtaining prior approval of the study protocol by the Institute Ethics Committee.

Preparation of porous 3D scaffolds: Chitosan, hydroxyapatite and polycaprolactone were supplied by Sigma Alderich, USA. The molecular weight and melt index of PCL were specified as 48,000-90,000 Da and 1.8 (g/10 min, 80°C). The molecular weight and density for CHT were 70,000-90,000 Da and 1.145 g/ml at 25°C, respectively. The molecular weight and particle size of HAP were 502.31 Da and <200 nm, respectively.

The pure chitosan, designated as 100CHT, was selected as matrix material for the preparation of the composites. The composites, CHT/HAP/PCL in the

ratio of 60/0/40, 60/10/30 and 60/15/25 designated as 40CHT/HAP, 30CHT/HAP/PCL and 25CHT/HAP/PCL, respectively, were prepared by freeze drying technique using a lyophilizer (Coolsafe 110-4, labogene, Lynge, Denmark). The chitosan was dissolved in 2mM acetic acid and PCL was dissolved in glacial acetic acid (Fisher Scientific, Mumbai, India) at 45°C using magnetic stirrer. The gel-like mixture was casted in a glass Petri dish and freeze dried at -80°C for 24 h. These samples were then neutralized in sodium hydroxide (NaOH, Hi-media, Mumbai, India) solution and washed with deionized water to remove any remaining NaOH. The scaffolds were cut into disc of 10 mm diameter and 2 mm thickness for *in vitro* studies. The scaffolds were again freeze dried and stored in dessicator.

Characterization of scaffolds

Morphology of scaffolds - The microstructure of the scaffolds was examined by STEREO-SCAN 360 scanning electron microscope (SEM, Cambridge Scientific Industries, MA, USA). The scaffolds was gold-coated and observed with SEM. Diameter of individual pores in the scaffolds were measured directly from the SEM images with 100X magnification using NIH Image J software (Dr Wayne Rasband, National Institutes of Health, Bethesda, MD, USA).

Porosity measurement of scaffolds - The porosity of scaffolds was measured by liquid displacement method[10]. The procedure for liquid displacement method was done as follows: the volume (V_0) and weight (W_0) of the samples were measured. Then, the sample was immersed into absolute ethanol until it was saturated by it. The sample was weighed again and noted as W_1. The porosity of the scaffold was calculated according to the following equation:

$$\text{Degree of porosity (\%)} = 100 \times (W_1 - W_0)/\rho V_0$$

(ρ represents the density of the ethanol).

In vitro degradation of scaffolds - The ability of scaffolds to degrade *in vitro* was studied using a lysozyme (Sigma Alderich, USA) degradation test. Lysozyme was used for the degradation study in the concentration similar to the circulatory level in human body (to mimic *in vivo* condition). The initial dry weight of the samples (W_0) was recorded. The samples were then placed in 0.1 M PBS (phosphate buffered saline) *p*H 7.4 containing 100 mg/l of lysozyme and incubated at 37°C. The samples were removed at 1, 3, 7, 14, 21, 28, 35, 42, 49 and 56 days to evaluate the weight loss. Per cent weight loss was calculated according to the following equation:

$$\text{\% Weight loss} = (W_0 - W_t) / W_0 \times 100$$

Where, W_0 is the starting dry weight and W_t is the dry weight at specified time.

Mechanical properties of scaffolds - Compressive properties of the scaffolds in wet state were evaluated with a Universal Testing Machine model H5KS (Tinius Olsen, Surrey, England, UK) with QMAT 5.37 professional software. The specimens were prepared as column of 20 mm in diameter and 10 mm in height. The scaffolds were immersed in PBS at *p*H 7.4 and 37°C for three days for complete hydration. The crosshead speed of the machine was set at 1mm/min with a load cell of 1 kilonewton until 50 per cent reduction in specimen height. The compressive strength and compressive modulus were determined from the stress-strain curve.

In vitro studies

Culture and seeding of the cells on scaffolds - Human BM was collected from the iliac crest of the patients undergoing stem cell transplantation after taking prior consent. hMSCs were isolated from BM on the basis of their property of plastic adherence. Briefly, 1-2 ml of BM was mixed with expansion media in 1:1 ratio and plated on the culture flasks. After incubation at 37°C for 24 h non-adherent cells were removed and fresh medium was added. In our experiments, hMSCs were cultured and expanded in a non-differentiating growth medium consisting of low glucose Dulbecco's modified Eagle medium (DMEM, Gibco, Life Technologies, USA) supplemented with 10 per cent foetal bovine serum (FBS) (0.03M, HyClone, Thermo scientific, USA), 2mM of L-glutamine (Gibco, Life Technologies, USA), 100 units/ml of penicillin and 0.1mg/ml of streptomycin (Gibco, Life Technologies, USA). Cells were grown in a 5 per cent CO_2 atmosphere at 37°C, and the medium was renewed every three days. Before confluence, cells were detached using trypsin-EDTA (Gibco, Life Technologies, USA) and passaged 1:3 into fresh culture flasks. All the experiments were performed with cells from passage 3-5. These cells were characterized using BD-LSR II (Becton-Dickinson, USA) and for their ability to differentiate into osteogenic, chondrogenic, and adipogenic lineages. The cells were positive for the cell surface markers CD105, CD29, (eBioscience, USA), CD73 and CD90 and negative for HLA Class II and CD34/45 (BD Pharmingen, USA).

hMSCs were grown to 80 per cent confluency, trypsinized, and re-suspended in cell expansion medium. hMSCs ($5x10^4$/20 µl) were seeded drop wise onto sterilized scaffold and incubated at 37 °C for 3 h to allow the cells to adhere, then 2 ml of medium was added to each well. The seeded scaffolds were cultured for four weeks with medium change thrice a week. For osteogenic differentiation, the cell expansion medium was supplemented with 10 nM dexamethasone, 50 µg/ml ascorbic acid- 2 phosphate and 10 mM beta-glycerophosphate obtained from Sigma, USA.

For cytotoxicity studies mouse lung fibroblast L929 cells were procured from National Centre for Cell Science, Pune, India. The cells were grown in DMEM (Gibco, Life Technologies, USA) supplemented with 10 per cent FBS and 100 units/ml of penicillin and 0.1mg/ml of streptomycin in a humidified incubator.

Cytotoxicity evaluation of scaffolds - The cytotoxicity of the scaffolds was assessed by [3-(4, 5-dimethylthiazol-2-yl)-2, 5-diphenyltetrazolium bromide] (MTT) assay. For cytotoxicity evaluation, we adopted the procedure from the ISO10993-5 standard test method[21]. Extraction media were prepared by immersing dry specimens in cell culture medium as described in literature[21]. L929 and hMSCs were separately cultured in 48 well ($5x10^4$/cells/well) plate in 500 µl extraction medium. After 24 h, MTT (Sigma, USA; 5 mg/ml in PBS) was added to each well and incubated for 3.5 h at 37°C. Then, dimethylsulphoxide (Sigma, USA) was added to each well to dissolve the formazan crystals produced by the activity of live cells and the coloured supernatant was read at 570 nm using plate reader (EL 800, Biotek, USA). In addition, standard calibration curve was made by MTT assay on known number of cells and the absorbance values were plotted against the known cell numbers. Metabolically active cell numbers were then determined using this standard curve based on their MTT absorbance.

Cell viability and distribution over scaffold - Viability and distribution of the cells seeded in the scaffold were examined after 7 and 14 days using Live/Dead staining kit (K501-100, Biovision, CA, USA). Scaffolds seeded with hMSCs ($5x10^4$ cells/scaffold) were washed with PBS and incubated with fluorescene di acetate (FDA) and propidium iodide (PI). After staining, the cells were visualized using Confocal Laser Scanning Microscope (CLSM) (TCS SP5, Leica, Germany).

Cell attachment and morphology - Cell attachment and morphology of cells seeded on the scaffolds were examined by scanning electron microscopy (SEM). Samples were collected at different time points and fixed with 2.5 per cent glutaraldehyde and stored at -80 °C. Samples were freeze dried using lyophilizer. Dried samples were mounted over aluminium stubs and sputter-coated with gold prior to imaging with a LEO 435 VP scanning electron microscope (Co-operation Zeiss, Leica, Cambridge, UK) at 5 KVA in secondary electron imaging mode.

Alkaline phosphatase (ALP) activity - The differentiation of hMSCs into osteoblasts in the scaffolds was evaluated by the measurement of alkaline phosphatase activity[22]. Briefly, the samples were harvested and freeze-thawed thrice in lysis buffer (1.0% Triton X-100) for cell lysis. An aliquot of the lysate was added to the ALP substrate buffer (equal parts of 20 mM *p*-nitrophenyl phosphate (1.5 M 2-amino-2-methyl-1-propanol from Sigma, USA, and 10 mM $MgCl_2$), and incubated for 30 min at 37 °C. Then, 3N NaOH was added to stop the enzymatic reaction. Hydrolysis of the substrate to *p*-nitrophenol was measured spectrophotometrically at 405 nm (EL 800, Biotek, USA).

Quantitative reverse transcription-PCR (qRT-PCR) analysis for the relative expression of osteoblasts specific genes, in differentiated osteoblasts derieved from hMSCs - The expression levels of collagen type 1 (CoLIA1), alkaline phosphatase (ALP), osteocalcin (OC), osteopontin (OP), transcription factor Cbfa 1 and osterix genes were quantitated[23]. Briefly, at each time point, total RNA was isolated using TRIzol (Life technologies, USA) as per the manufacturer's protocol. RNA samples were treated with Dnase I (Sigma; 1 U/µg RNA) for 25 min at room temperature to remove residual genomic DNA. The concentration of the purified RNA was quantified using nanospectrophotometer (P300, Implen GmbH, Germany). cDNA was transcribed using 200U of M-MLV reverse transcriptase, 0.5 mM dNTPs and 12.5 ng/ml oligo-dT and 40 U of RNase inhibitor RNasin (all from Promega, USA). The gene specific primers were custom made (Sigma, Bangalore, India) and are summarized in Table I. Reactions were carried out using SYBR Green Super Mix (KAPA Biosystems, Capetown, South Africa) in a final volume of 10 µl with 0.3 µM of each primer. Relative gene expression was quantified by $2^{-\Delta\Delta Ct}$ method[24] in which the accumulated PCR products of each of the genes examined was normalized to the housekeeping gene *GAPDH* in the corresponding samples. ΔCt was obtained by subtracting the Ct_{GAPDH} from Ct_{target} (ΔCt =

Table I. Primer sequence used for qPCR amplification

Sl. No.	Gene	Primer sequence	Amplicon length (bp)	Annealing temperature (°C)
1	*ALP*	**F-** GGACATGCAGTACGAGCTGA **R-** CCACCAAATGTGAAGACGTG	282	55
2	*RUNX2*	**F-** AGAGGTACCAGATGGGACTGTGGTT **R-** GGTAGCTACTTGGGGAGGATTTGTG	199	55
3	*COLlA1*	**F-** AGGACAAGAGGCATGTCTGGTT **R-** CCCTGGCCGCCATACTC	70	55
4	Osteopontin *(SPP1)*	**F-** AGGCATCACCTGTGCCATACCA **R-** ACTTGGAAGGGTCTGTGGGGCT	154	55
5	Osteocalcin *(BGLAP)*	**F-** GGCAGCGAGGTAGTGAAGAG **R-** CTCACACACCTCCCTCCTG	102	55
6	Osterix *(SP7)*	**F-** TGCACTCTCCCTGCCAGACCTC **R-** AACGGGTCCCAAGGAGCCAGG	99	55
7	*GAPDH*	**F-** GCAGGGGGGAGCCAAAAGGG **R-** TGCCAGCCCCAGCGTCAAAG	200	55

ALP, alkaline phosphatase; GAPDH, glyceraldehyde phosphate dehydrogenase; COL1A1, collagen type 1, RUNX2, runt related transcription factor 2

$Ct_{Target} - Ct_{GAPDH}$) and ΔΔCt was obtained by subtracting $\Delta Ct_{uninduced\ cells}$ from $\Delta Ct_{induced\ cells}$ ($\Delta\Delta Ct = \Delta Ct_{induced\ cells} - \Delta Ct_{un\ induced\ cells}$). Negative controls were used as no template cDNA reactions and melting curves were used to confirm the results.

The relative quantitative qPCR experiments were performed by using a Realplex 4 epgradient Mastercycler (Eppendorf, Hamburg, Germany) according to the manufacturer's instructions.

Statistical analysis: All statistical analyses were performed using GraphPad Software (La Jolla, CA, USA). All measurements were collected in triplicates and expressed as means ± standard deviation, unless otherwise noted. In cases where statistical comparisons were made between three or more groups of data, a one-way analysis of variance was performed. In cases where only two sets of data were compared, a Student unpaired t test was performed.

Results

Microstructure of scaffolds: The external morphology of scaffolds was studied by SEM (Fig. 1). Scaffolds were seen to be highly porous with open and interconnected pores surrounded by thin polymer walls. The microstructure of the scaffolds did not seem to vary from one another since the treatment given to each was similar. The composition did not affect the pore size and porosity of the scaffolds. Pore size and porosity data of the scaffolds are given in Table II.

In vitro degradation of scaffolds: Fig. 2a shows the weight loss of scaffolds as a function of soaking time in PBS. The 100CHT showed maximum weight loss (91%), followed by 40CHT/HAP (70%), 30CHT/HAP/PCL (34%) and 25CHT/HAP/PCL (30%) at the end of 56 days. After enzymatic degradation for 56 days, change in morphology of the 100CHT and 40CHT/HAP scaffolds was observed (Fig. 2b). The scaffold 30CHT/HAP/PCL and 25CHT/HAP/PCL remained in the original shape, indicating that these scaffolds had good structural stability.

Mechanical properties of scaffolds: The compressive stress-strain curves of the pure and composite scaffolds are shown in Fig. 3, and the data of compressive strength and compressive modulus are given in Table III. As expected, 100CHT scaffold showed low compressive strength and modulus. The mixing of HAP with CHT significantly improved the compressive strength and compressive modulus of 40CHT/HAP. Further addition of PCL (10%) to the 40CHT/HAP showed no significant difference in the compressive strength and modulus of the 30CHT/HAP/PCL composite scaffold. Increasing the PCL content to 15 per cent dramatically increased the compressive strength ($P<0.01$) and compressive modulus ($P<0.001$) of 25CHT/HAP/PCL composite scaffold.

Cytotoxicity of the scaffolds: The cytotoxicity of 3D composite scaffolds was tested by quantitative analysis

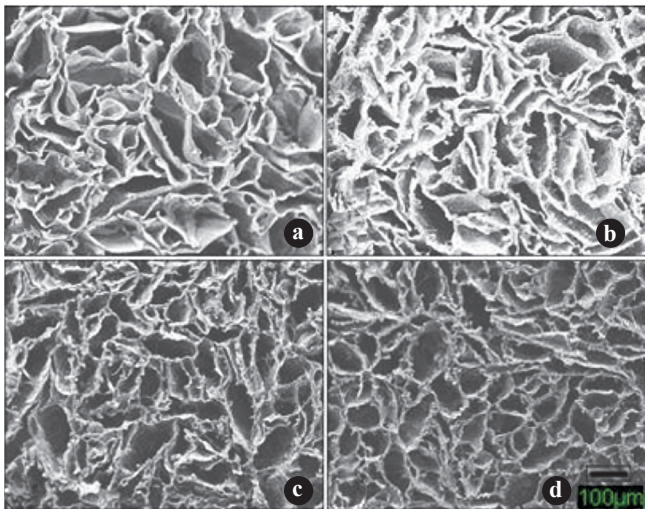

Fig. 1. Representative scanning electron microscope (SEM) photomicrographs illustrating the open porous structure of the scaffolds with homogenous distribution of pores. **(a)** 100CHT **(b)** 40CHT/HAP **(c)** 30CHT/HAP/PCL and **(d)** 25CHT/HAP/PCL (Scale bar 100µm).

using the MTT assay. The absorbance values of test samples after exposure to the extraction medium for 24 h were similar to the negative control (Table IV). Absorbance values correspond to the number of metabolically active cells. Thus our results (Fig. 4) indicated that the metabolic activity of L929 and hMSCs cells was not inhibited by the extraction medium. From the quantitative scores, it was concluded that the extracts of the scaffolds demonstrated no cytotoxic reactivity in this test.

Viability and distribution of hMSCs in scaffolds: The viability and distribution of hMSCs on scaffolds were visualized using CLSM after 7 and 14 days of cells seeding, which depicted a high ratio of living cells on all scaffold compositions. As shown in Fig. 5, >90 per cent cells were live, randomly distributed within the porous 3D scaffolds. hMSCs were connected to each other and formed a cell network across the surface of the scaffolds. The cells proliferated and their number increased from day 7 to day 14 (Fig. 6). Up to 14 days of cultivation, no large difference in the viability and morphology was observed. Cells were more evenly distributed over 30CHT/HAP/PCL and 25CHT/HAP/PCL scaffolds compared to 100CHT and 40CHT/HAP scaffolds.

Attachment and morphology of hMSCs on scaffolds: After seven days of cell seeding, cells adhered and spreaded over the porous scaffold surface and merged completely with each other so that intercellular connections were not visible (Fig. 7). After 14 days it was found that cells were merged and formed a complete cellular layer on the surface of the scaffolds, so that the surface was almost covered and only a few pores were visible and a few cells migrated inside the pores (Fig. 8). This preliminary experiment suggested that CHT and composites scaffolds had biocompatibility for hMSCs attachment. These findings were supported by simultaneous CLSM imaging.

Specific alkaline phosphatase activity of hMSCs differentiated into osteoblasts on scaffolds: ALP is an enzyme produced by differentiating osteoblasts. ALP activity can serve as a marker indicating differentiation of hMSCs toward the osteoblastic lineage. In un-induced culture condition (Fig. 9a), the ALP activity of hMSCs on scaffolds and tissue culture plastic surface (TCPS) slightly increased over the whole culture period of 28 days. In osteogenic condition (Fig. 9b) the ALP activity of the hMSCs, increased progressively over time from day 3 to 28. ALP activity of hMSCs in osteogenic condition was significantly higher on all scaffolds compared to TCPS ($P<0.01$). Among the scaffolds, 25CHT/HAP/PCL showed slightly higher ALP activity. hMSCs on TCPS showed a decline in ALP activity after day 14.

qPCR analysis for relative expression of osteoblasts specific genes, in osteoblasts derived from differentiation of hMSCs: Results obtained from

Table II. Pore parameters of scaffolds, determined by scanning electron microscopy and liquid displacement methods

Scaffold samples	Pore size interval (µm)	Pore size (µm)	Porosity (%)
100CHT	50-325	140 ± 59	84 ± 3.9
40CHT/HAP	50-270	149 ± 47	83 ± 5.5
30CHT/HAP/PCL	30-260	140 ± 53	81 ± 1.8
25CHT/HAP/PCL	30-270	141 ± 47	80 ± 3.1

Data represent mean ± SD of five independent experiments
CHT, chitosan; HAP, hydroxypatite; PCL, polycarpolactone

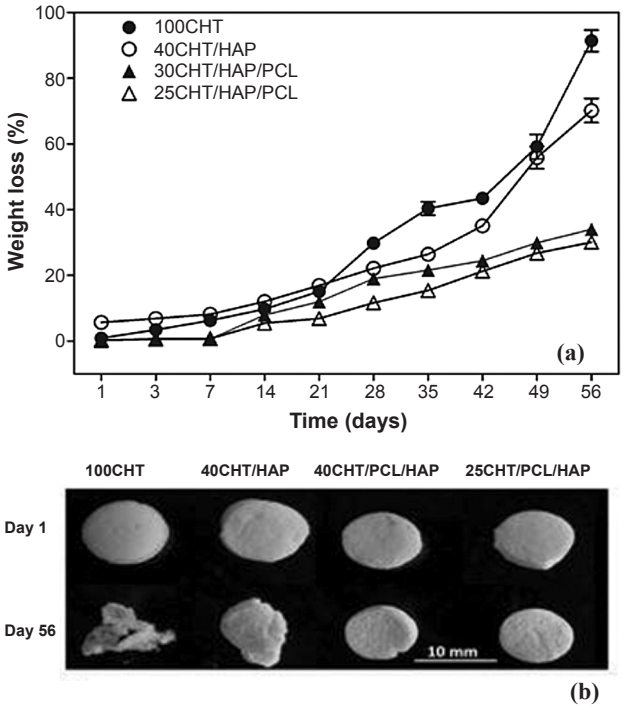

Fig. 2(a) Degradation kinetics of 100CHT, 40CHT/HAP, 30CHT/HAP/PCL and 25CHT/HAP/PCL scaffolds. Data represent mean value of five independent experiments, **(b)** Digital images showing the morphology of scaffolds after *in vitro* enzymatic treatment at days 1 and 56.

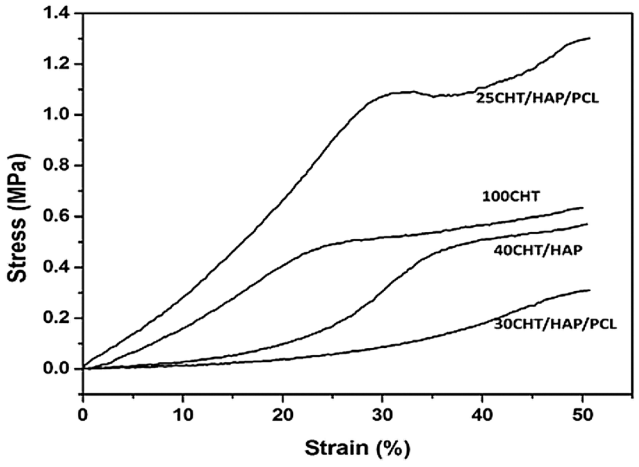

Fig. 3. Representative compression stress-strain curves of pure and composite scaffolds.

qRT-PCR were quantitative and presented as a 'fold change' in mRNA levels in differentiated hMSCs when compared to undifferentiated hMSCs (Fig. 10). A value greater than 1 corresponds to a higher gene expression by differentiated hMSCs. Differentiation

Table III. Mechanical properties of porous scaffolds

Scaffold samples	Compressive strength (MPa)	Compressive modulus (KPa)
100CHT	0.28 ± 0.06	2 ± 0.05
40CHT/HAP	0.52 ± 0.04**	17 ± 3.1*
30CHT/HAP/PCL	0.56 ± 0.07	32 ± 3.6
25CHT/HAP/PCL	1.30 ± 0.06††	41 ± 3.6†††

Data represent mean ± SD of five independent experiments
Abbreviations as given in Table II
*P<0.05, **<0.01, compared with respective 100CHT
††P<0.01, †††<0.001 compared with respective 30CHT/HAP/PCL

of osteogenic-induced hMSC on scaffolds and TCPS was further demonstrated by an increase in the relative expression of the osteoblasts specific genes. The relative expression of osteoblasts specific genes on scaffolds was several fold upregulated compared to TCPS. A slightly higher maximal expression of genes was detected on scaffold 25CHT/HAP/PCL compared to 30CHT/HAP/PCL, 40CHT/HAP and 100CHT scaffolds (found on day 28). However, the maximum OP expression was detected on 30CHT/HAP/PCL.

Discussion

In this study we prepared porous foam like scaffolds with average pore size of 140 µm, which could support cell penetration, migration, tissue in-growth and vascularisation as reported in the literature[25,26] and the average porosity of the scaffold was 82 per cent, which was in the range of the porosity of the trabecular bone (50-90%). Determination of a balance between mechanical strength and porosity is crucial. As porosity and mean pore sizes increase, mechanical strength is decreased. In this study, by fabricating scaffolds with optimal pore size and porosity it was possible to maintain the mechanical strength of scaffold. The porous 100CHT scaffolds were tissue biocompatible but mechanically weak and unable to maintain structure integrity as also reported in literature[11]. It is because of the hydrophilic nature of the CHT. In aqueous medium CHT absorbs a lot of water and swells resulting in poor structural stability and low mechanical strength. To overcome this problem we doped CHT with PCL and HAP. PCL being hydrophobic decreased the total water absorption and swelling and HAP as a filler strengthened the scaffold. The resulting composite

Table IV. Cell proliferation studies on scaffolds.

Sample	Number of cells (counts) seeded		Number of cells (counts) after 24 h	
	L929	hMSC	L929	hMSC
Negative control	50000	50000	70054	50940
100CHT	50000	50000	68737	49832
40CHT/HAP	50000	50000	66052	49654
30CHT/HAP/PCL	50000	50000	64438	49750
25CHT/HAP/PCL	50000	50000	69134	49965
Positive control	50000	50000	-	-

Abbreviations as given in Table II

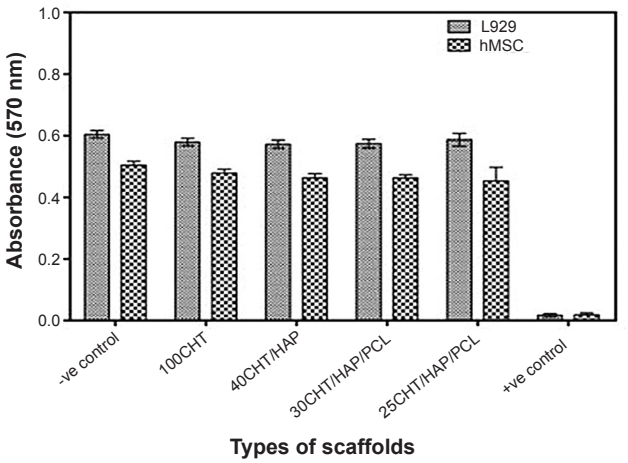

Fig. 4. Determination of cytotoxicity of scaffolds by MTT assay. The viability of mouse lung fibroblast cell line L929 and hMSCs was evaluated that had been cultured for 24 h with the extraction media from the specimens. Data represent mean ± SD of five independent experiments.

25CHT/HAP/PCL scaffold showed better compressive strength compared to pure 100CHT scaffold, which was very close to the lower limit of compressive strength of trabecular bone (2-10 MPa)[6]. Thus, incorporation of HAP and PCL into composite scaffolds in specific ratios could improve their mechanical properties.

In *in vitro* degradation study, it was found that the weight loss of the scaffolds increased gradually. The degradation rate of 100CHT and 40CHT/HAP scaffold was high compared to the composite scaffolds, 30CHT/HAP/PCL and 25CHT/HAP/PCL. This result was expected as CHT is hydrophilic and susceptible to lysozyme[8]. The result suggested that presence of PCL decreased degradation of the composite scaffold because of its being hydrophobic and semi-crystalline material with a slow *in vitro* hydrolytic degradation rate[27]. Pure 100CHT scaffolds were found to degrade >90 per cent and disintegrated upon handling. In contrast, the composite 30CHT/HAP/PCL and 25CHT/HAP/PCL scaffolds retained their original shape, despite evidence of degradation from weight loss measurements.

The MTT assay showed that all the scaffolds prepared in this study were nontoxic and biocompatible. The polymer composition and the method of fabrication also play an important role in cell biocompatibility. Our results showed overall good viability of the cells

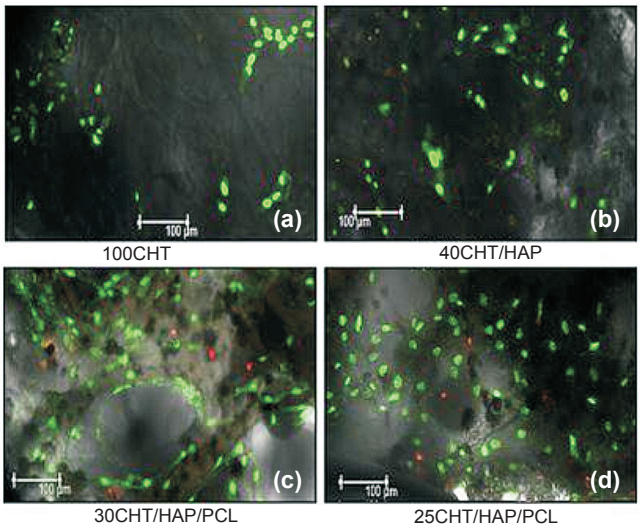

Fig. 5. Confocal laser microscopic images of hMSCs grown on scaffolds after seven days **(a)** cells were randomly distributed and forming patch on 100CHT, **(b)** hMSCs adhered and attained fibroblastic morphology on 40CHT/HAP, **(c, d)** Cells were more evenly distributed over 30CHT/HAP/PCL and 25CHT/HAP/PCL, covered whole surface of the scaffold. Viability and distribution of cells were detected using fluorescence markers that allowed life/death stain (FDA /PI): dead cells were stained red whereas viable cells were stained green (Magnification 10X).

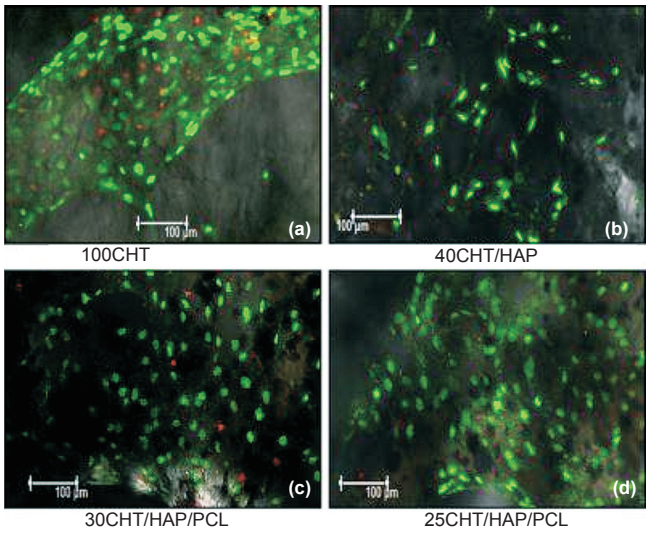

Fig. 6. Confocal laser microscopic images of hMSCs grown on scaffolds after 14 days. **(a)** Cells proliferated and form a large patch on 100CHT, **(b)** Cells increased in number and evenly distributed on 40CHT/HAP, **(c, d)** Cells proliferated and their number increased from day 7 to 14. Cells were connected to each other and formed a cell network across the surface of 30CHT/HAP/PCL and 25CHT/HAP/PCL scaffolds. Viability and distribution of cells were detected using fluorescence markers that allowed life/death stain (FDA /PI): dead cells were stained red whereas viable cells were stained green. The qualitative image analysis revealed that a larger number of cells stayed viable throughout the entire culture period. (Magnification 10X).

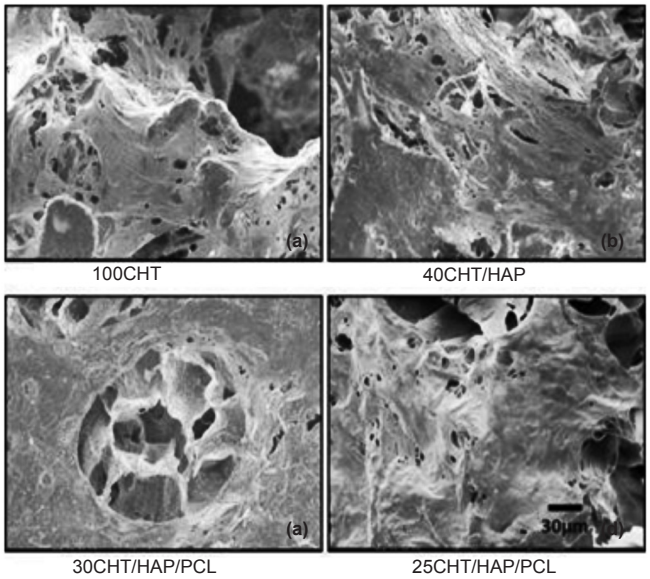

Fig. 7. Scanning electron microscope (SEM) images of human mesenchymal stem cells (hMSCs) grown on 100CHT, 40CHT/HAP, 30CHT/HAP/PCL and 25CHT/HAP/PCL scaffolds after seven days. The hMSCs adhered and spreaded on scaffolds (Scale bar 30 µm).

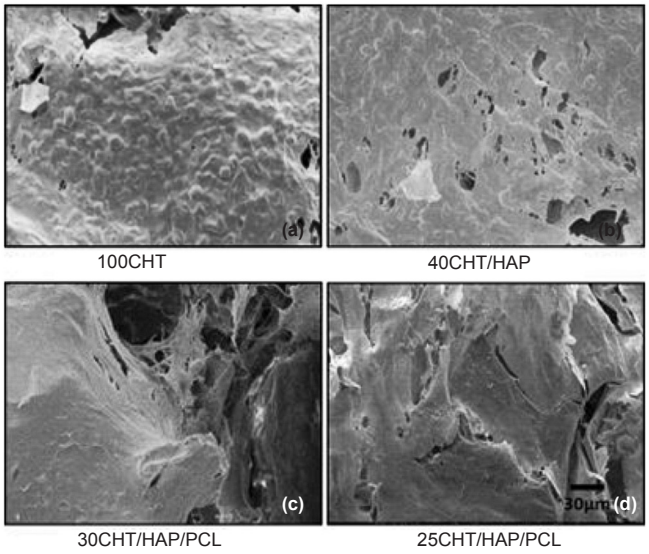

Fig. 8. SEM images of hMSCs grown on 100CHT, 40CHT/HAP, 30CHT/HAP/PCL and 25CHT/HAP/PCL scaffolds after 14 days. At 14 days, cells grew and merged to form a cell sheet, got enlarged and migrated into the pores of scaffolds. (Scale bar 30 µm).

indicating that these scaffolds were free of toxic chemicals and suitable for *in vitro* and *in vivo* studies.

The ability of hMSCs to differentiate into osteogenic lineage is the key to the use of these cells to improve bone formation. The present study showed that the scaffolds supported hMSCs attachment, proliferation and differentiation. SEM images showed that the large surface area of the porous scaffolds allowed hMSCs to adhere, spread and grow on the scaffolds. It has been shown that chitosan coating on 2-D polymeric films or 3-D polymer scaffolds may affect the attachment, proliferation and differentiation of cells[28]. The flat morphology, and excellent spreading in and around the interconnected porous structure, indicated strong cellular adhesion and growth of cells. The 3D structure of the scaffold might have been responsible for the attachment of hMSCs and differentiation into osteoblasts[29].

The parallel investigations of cell viability and distribution carried out by CLSM revealed proliferation of the cells on the scaffolds with clear spreading and good morphology. Live dead staining and CLSM showed that >90 per cent hMSCs were live and distributed throughout the scaffolds. This indicates that the pores of the scaffolds are interconnected and large enough for cells to penetrate and colonize the porous structure.

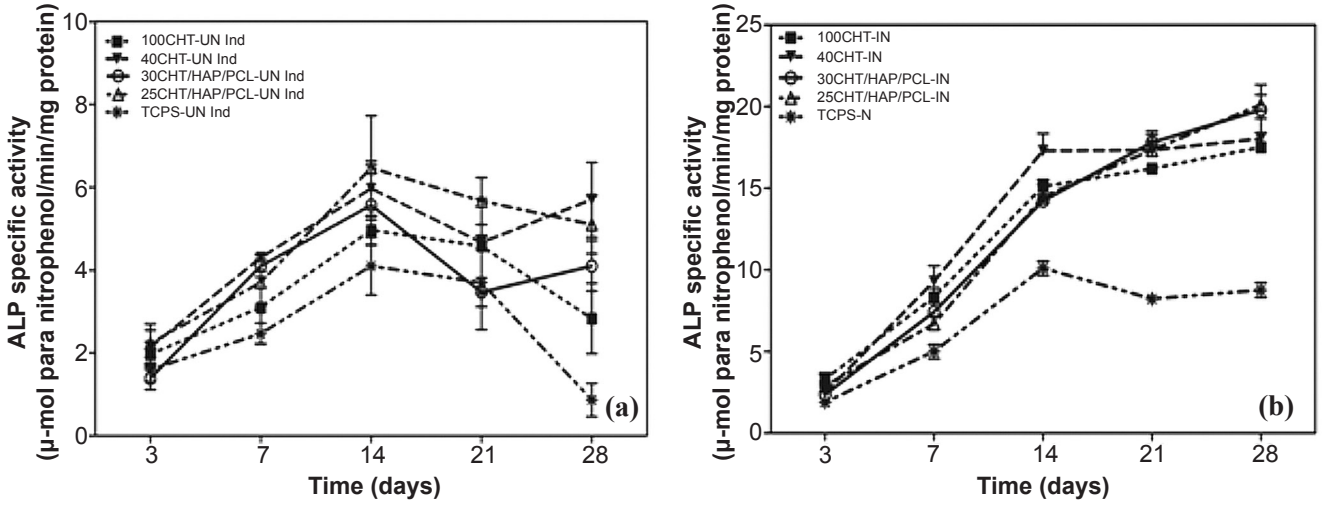

Fig. 9. Determination of alkaline phosphatase (ALP) activity of hMSCs over 100CHT, 40CHT/HAP, 30CHT/HAP/PCL, 25CHT/HAP/PCL scaffolds and tissue culture plastic surface (TCPS) under **(a)** un-induced culture condition and **(b)** induced culture condition. ALP activity of hMSCs in the cell-scaffold constructs was assessed during four weeks of culture. Values represent mean ± SD of five independent experiments.

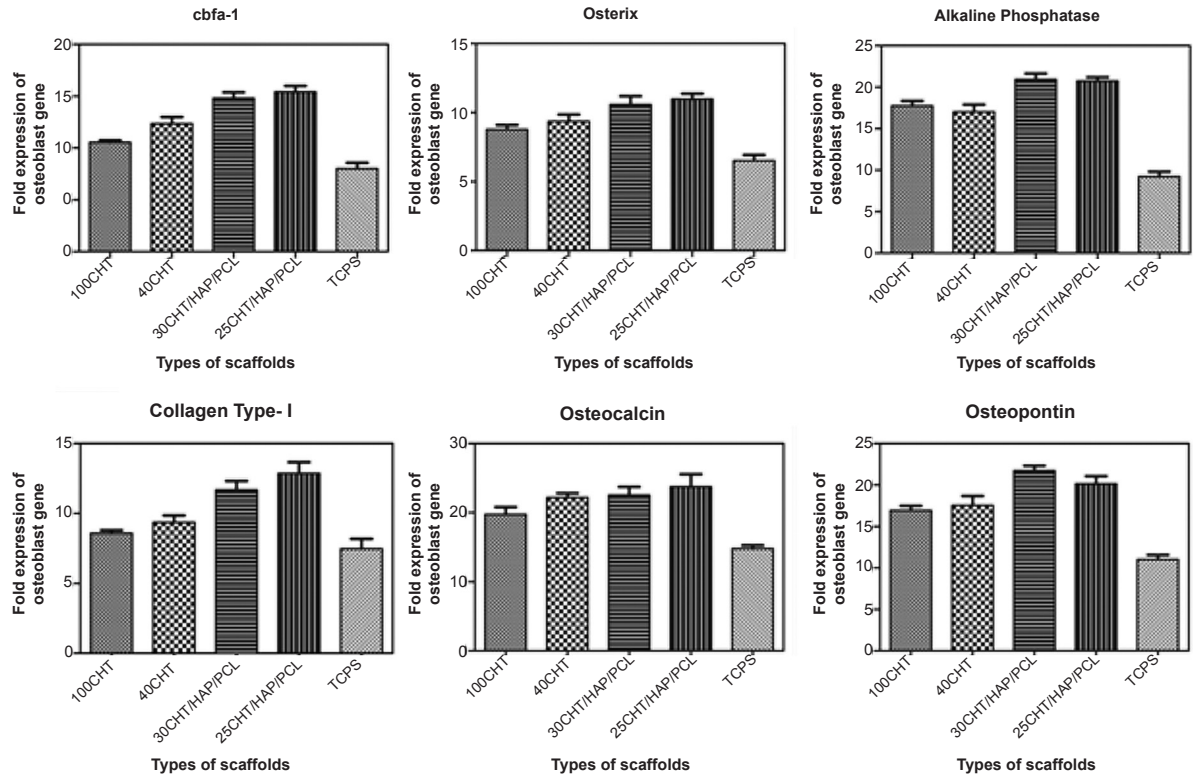

Fig. 10. Real-time quantitative reverse transcriptase PCR analysis of the expression levels of osteogenic markers. Expression levels of cbfa-1, osterix, alkaline phosphatase, collagen type I, osteocalcin, and osteopontin genes were determined in hMSCs cultured over 100CHT, 40CHT/HAP, 30CHT/HAP/PCL and 25CHT/HAP/PCL scaffolds and tissue culture plastic surface (TCPS) under osteogenic and non-osteogenic culture conditions for 28 days. Expression of the house-keeping gene *GAPDH* served as an internal control. Values represent mean ± SD of six independent experiments.

ALP is an enzyme expressed by MSCs during osteogenesis and is a well-defined marker of osteoblastic lineage[30]. Surface roughness of the scaffold material also induces differentiation of hMSCs into osteoblasts. Thein-Han *et al*[16] has demonstrated that presence of HAP nanoparticles in CHT/nHAP nanocomposite scaffolds influence cytoskeleton organization, which regulates cellular signal transduction, cell differentiation and gene expression. In this study, we also found that hMSCs cultured over composite scaffolds showed higher specific ALP activity than those cultured over pure CHT scaffolds and TCPS.

The expression of osteoblasts specific genes was multiple folds in induced hMSCs compared to the un-induced hMSCs. However, in non-osteogenic conditions the cells over 3D scaffolds showed enhanced osteoblastic genes expression compared to cells cultured on TCPS. This indicated that the 3D geometry of scaffolds also favoured osteogenic differentiation of hMSCs. It might be because of the inherent osteoinductivity and osteoconductivity of the CHT and HAP present in the scaffold. Nair *et al*[31] showed the same findings with silica coated HAP scaffolds. In addition, results of a cell culture study showed both enhanced proliferation and differentiation of rat calvarial osteoblasts on bone cement scaffold[32]. After comparing all the properties of scaffolds it was found that the novel 25CHT/HAP/PCL biomedical composite scaffold had good mechanical strength, optimum pore size and porosity, required degradability, cell biocompatibility and osteo-inductivity.

In conclusion, the present study demonstrated the feasibility of using the freeze drying technique to fabricate 3D biocomposite scaffolds. The addition of HAP and PCL to CHT improved the compressive strength while maintaining high porosity with interconnected pores. The *in vitro* biocompatibility study of the scaffolds showed that the polycaprolactone did not affect attachment, proliferation and differentiation on the scaffolds. The 25CHT/HAP/PCL composite scaffold possessed the inherent physiochemical and efficient mechanical and biocompatible characteristics. The 25CHT/HAP/PCL biocomposite appears to be potential scaffolds as an off the shelf, synthetic, resorbable bone graft substitute for bone regeneration.

References

1. Meinel L, Fajardo R, Hofmann S, Langer R, Chen J, Synder B, *et al*. Silk implants for the healing of critical size bone defects. *Bone* 2005; *37* : 688-98.
2. Amini AR, Laurencin CT, Nukavarapu SP. Bone tissue engineering: recent advances and challenges. *Crit Rev Biomed Eng* 2012; *40* : 363-408.
3. Brydone AS, Meek D, Maclaine S. Bone grafting, orthopaedic biomaterials, and the clinical need for bone engineering. *Proc Inst Mech Eng H* 2010; *224* : 1329-43.
4. Ko J, Kolehmainen K, Ahmed F, Jun MB, Willerth SM. Towards high throughput tissue engineering: development of chitosan-calcium phosphate scaffolds for engineering bone tissue from embryonic stem cells. *Am J Stem Cells* 2011; *1* : 81-9.
5. Shor L, Guceri S, Chang R, Gorden J, Kang Q, Hartsock L, *et al*. Precision extruding deposition (PED) fabrication of polycaprolactone (PCL) scaffolds for bone tissue engineering. *Biofabrication* 2009; *1* : 015003.
6. Hutmacher DW. Scaffolds in tissue engineering bone and cartilage. *Biomaterials* 2000; *21* : 2529-43.
7. Biazar E, Heidari Keshel S, Rezaei Tavirani M, Jahandideh R. Bone formation in calvarial defects by injectable nanoparticular scaffold loaded with stem cells. *Expert Opin Biol Ther* 2013; *13* : 1653-62.
8. Pattnaik S, Nethala S, Tripathi A, Saravanan S, Moorthi A, Selvamurugan N. Chitosan scaffolds containing silicon dioxide and zirconia nano particles for bone tissue engineering. *Int J Biol Macromol* 2011; *49* : 1167-72.
9. Jiang T, Abdel-Fattah WI, Laurencin CT. *In vitro* evaluation of chitosan/poly(lactic acid-glycolic acid) sintered microsphere scaffolds for bone tissue engineering. *Biomaterials* 2006; *27* : 4894-903.
10. Han J, Zhou Z, Yin R, Yang D, Nie J. Alginate-chitosan/hydroxyapatite polyelectrolyte complex porous scaffolds: Preparation and characterization. *Int J Biol Macromol* 2010; *46* : 199-205.
11. Li Z, Ramay HR, Hauch KD, Xiao D, Zhang M. Chitosan-alginate hybrid scaffolds for bone tissue engineering. *Biomaterials* 2005; *26* : 3919-28.
12. Ketelaars AAJ, Papantoniou Y. Nakayama K. Analysis of the density and the enthalpy of poly(e-caprolactone) polycarbonate blends: Amorphous phase compatibility and the effect of secondary crystallization. *J Appl Polym Sci* 1997; *66* : 921-7.
13. Montazeri N, Jahandideh R, Biazar E. Synthesis of fluorapatite-hydroxyapatite nanoparticles and toxicity investigations. *Int J Nanomed* 2011; *6* : 197-201.
14. Landi E, Valentini F, Tampieri A. Porous hydroxyapatite/gelatine scaffolds with ice-designed channel-like porosity for biomedical applications. *Acta Biomater* 2008; *4* : 1620-6.
15. Xie J, Li X, Xia Y. Putting electrospun nanofibers to work for biomedical research. *Macromol Rapid Commun* 2008; *29* : 1775-92.
16. Thein-Han WW, Misron RD. Biomimetic chitosan-nanohydroxyapatite composite scaffolds for bone tissue engineering. *Acta Biomater* 2009; *5* : 1182-97.
17. Rohner D, Hutmacher DW, Cheng TK, Oberholzer M, Hammer B. *In vivo* efficacy of bone-marrow-coated polycaprolactone scaffolds for the reconstruction of orbital defects in the pig. *J Biomed Mater Res B Appl Biomater* 2003; *66* : 574-80.

18. Williams JM, Adewunmi A, Schek RM, Flanagan CL, Krebsbach PH, Feinberg SE, *et al*. Bone tissue engineering using polycaprolactone scaffolds fabricated via selective laser sintering. *Biomaterials* 2005; *26* : 4817-27.

19. Rastegar F, Shenaq D, Huang J, Zhang W, Zhang BQ, He BC, *et al*. Mesenchymal stem cells: molecular characteristics and clinical applications. *World J Stem Cells* 2010; *2* : 67-80.

20. Brown PT, Handorf AM, Jeon WB, Li WJ. Stem cell-based tissue engineering approaches for musculoskeletal regeneration. *Curr Pharm Des* 2013; *19* : 3429-45.

21. Sutthiphong S, Pavasant P, Supaphol P. Electrospun 1,6-diisocyanatohexane-extended poly(1,4-butylene succinate) fiberÂ mats and their potential for use as bone scaffolds. *Polymer* 2009; *50* : 1548-58.

22. Costa-Pinto AR, Salgado AJ, Correlo VM, Sol P, Bhattacharya M, Charbord, P, *et al*. Adhesion, proliferation, and osteogenic differentiation of a mouse mesenchymal stem cell line (BMC9) seeded on novel melt-based chitosan/polyester 3D porous scaffolds. *Tissue Eng Part A* 2008; *14* : 1049-57.

23. Osyczka AM, Leboy PS. Bone morphogenetic protein regulation of early osteoblast genes in human marrow stromal cells is mediated by extracellular signal-regulated kinase and phosphatidylinositol 3-kinase signaling. *Endocrinology* 2005; *146* : 3428-37.

24. Rao X, Huang X, Zhou Z, Lin X. An improvement of the 2ˆ(-delta delta CT) method for quantitative real-time polymerase chain reaction data analysis. *Biostat Bioinforma Biomath* 2013; *3* : 71-85.

25. Guarino V, Causa F, Netti PA, Ciapetti G, Pagani S, Martini D, *et al*. The role of hydroxyapatite as solid signal on performance of PCL porous scaffolds for bone tissue regeneration. *J Biomed Mater Res B Appl Biomater* 2008; *86* : 548-57.

26. Zmora S, Glicklis R, Cohen S. Tailoring the pore architecture in 3-D alginate scaffolds by controlling the freezing regime during fabrication. *Biomaterials* 2002; *23* : 4087-94.

27. Salerno A, Guarnieri D, Iannone M, Zeppetelli S, Netti PA. Effect of micro- and macroporosity of bone tissue three-dimensional-poly(epsilon-caprolactone) scaffold on human mesenchymal stem cells invasion, proliferation, and differentiation *in vitro*. *Tissue Eng Part A* 2010; *16* : 2661-73.

28. Zhensheng Li, Hassna R. Ramay, Kip D. Hauch, Demin Xiao, Miqin Zhanga. Chitosan-alginate hybrid scaffolds for bone tissue engineering. *Biomaterials* 2004; *26* : 3919-28.

29. George J, Kuboki Y, Miyata T. Differentiation of mesenchymal stem cells into osteoblasts on honeycomb collagen scaffolds. *Biotechnol Bioeng* 2006; *95* : 404-11.

30. Wu H, Wan Y, Dalai S, Zhang R. Response of rat osteoblasts to polycaprolactone/chitosan blend porous scaffolds. *J Biomed Mater Res A* 2010; *92* : 238-45.

31. Nair MB, Bernhardt A, Lode A, Heinemann C, Thieme S, Hanke T, *et al*. A bioactive triphasic ceramic-coated hydroxyapatite promotes proliferation and osteogenic differentiation of human bone marrow stromal cells. *J Biomed Mater Res A* 2009; *90* : 533-42.

32. Reinstorf A, Ruhnow M, Gelinsky M, Pompe W, Hempel U, Webzek KW, *et al*. Phosphoserine--a convenient compound for modification of calcium phosphate bone cement collagen composites. *J Mater Sci Mater Med* 2004; *15* : 451-5.

Reprint requests: Dr Sujata Mohanty, Stem Cell Facility, All India Institute of Medical Sciences,
Ansari Nagar, New Delhi 110 029, India
e-mail: drmohantysujata@gmail.com